Human Molecular Genetics, 2001, Vol. 10, No. 22 **2593–2601**

Severe neural tube defects in the *loop-tail* mouse result from mutation of *Lpp1*, a novel gene involved in floor plate specification

Jennifer N. Murdoch, Kit Doudney[1], Caroline Paternotte, Andrew J. Copp* and Philip Stanier[1]

Neural Development Unit, Institute of Child Health, University College London, 30 Guilford Street, London WC1N 1EH, UK and [1]Department of Maternal and Fetal Medicine, Institute of Reproductive and Developmental Biology, Imperial College School of Medicine, Hammersmith Campus, London W12 0NN, UK

Received August 2, 2001; Revised and Accepted August 23, 2001

Neural tube defects (NTD) are clinically important congenital malformations whose molecular mechanisms are poorly understood. The *loop-tail* (*Lp*) mutant mouse provides a model for the most severe NTD, craniorachischisis, in which the brain and spinal cord remain open. During a positional cloning approach, we have identified a mutation in a novel gene, *Lpp1*, in the *Lp* mouse, providing a strong candidate for the genetic causation of craniorachischisis in *Lp*. *Lpp1* encodes a protein of 521 amino acids, with four transmembrane domains related to the *Drosophila* protein *strabismus*/*van gogh* (*vang*). The human orthologue, *LPP1*, shares 89% identity with the mouse gene at the nucleotide level and 99% identity at the amino acid level. *Lpp1* is expressed in the ventral part of the developing neural tube, but is excluded from the floor plate where *Sonic hedgehog* (*Shh*) is expressed. Embryos lacking *Shh* express *Lpp1* throughout the ventral neural tube, suggesting negative regulation of *Lpp1* by *Shh*. Our findings suggest that the mutual interaction between *Lpp1* and Shh may define the lateral boundary of floor plate differentiation. Loss of *Lpp1* function disrupts neurulation by permitting more extensive floor plate induction by Shh, thereby inhibiting midline bending of the neural plate during initiation of neurulation.

INTRODUCTION

Closure of the neural tube is essential for normal development of the brain and spinal cord. Failure of neural tube closure is among the commonest of human congenital malformations, with a prevalence of ~1 per 1000 pregnancies (1). In craniorachischisis, the most severe type of neural tube defect (NTD), almost the entire brain and spinal cord remain open (Fig. 1A and B), as a result of a failure to initiate closure at the start of neurulation (2,3). Craniorachischisis comprises 10–20% of human NTD (4–6), and leads to death around the time of birth. Although the aetiology of human craniorachischisis is unknown, there is a close similarity between this defect and the phenotype of the *loop-tail* (*Lp*) mouse mutant (7,8). This resemblance has prompted a series of studies, over a 50 year period (7–10), aimed at determining the developmental basis of craniorachischisis and identifying the causative gene in the *Lp* mouse.

Lp is one of only two known gene mutations that disrupt the onset of mouse neural tube closure, which occurs at the hindbrain–cervical boundary in embryos with six to seven somites. This initial neurulation event, so-called 'Closure 1', is essential for the subsequent closure of the entire spine and much of the brain: hence, the severe NTD phenotype resulting from failure of Closure 1 (2). The other gene known to be essential for Closure 1 is *circletail* (*Crc*), a recently described mutation, with a closely similar phenotype to *Lp* (11). The two mutations are not allelic, and yet they interact in *Lp*/*Crc* compound heterozygotes to produce craniorachischisis closely resembling the phenotype of the *Lp* and *Crc* single homozygotes (12). These findings suggest the existence of a developmental pathway, involving the *Lp* and *Crc* genes, that is critical in regulating the onset of neurulation.

A clue to the underlying developmental defect in *Lp* is the finding of an enlarged presumptive floor plate region in the midline neural plate of *Lp* homozygous embryos (13). In normal circumstances, neurulation at the site of Closure 1 involves bending of the neural plate solely in the midline (14). Enlargement of the floor plate region in *Lp/Lp* embryos, prior to the onset of neural tube closure at embryonic day (E) 8.5, disrupts midline bending so that the neural folds are more widely spaced apart than normal. This defect appears to lead directly to the failure of neural tube closure (13). Subsequently, the floor plate differentiates as an abnormally broad structure in the posterior region of *Lp/Lp* embryos, with an abnormally extensive expression domain of the floor plate marker, *Sonic hedgehog* (*Shh*).

Although the molecular mechanism responsible for enlargement of the presumptive floor plate region in *Lp* has not been determined, one possibility is a recruitment of cells into the floor plate from more lateral regions of the neural plate. According to this idea, the normal function of the *Lp* gene product might be to restrict the lateral extent of floor plate differentiation. In the present study, we report the outcome of a positional cloning project to identify candidate genes for *Lp*. We have identified a mutation in a novel gene, named *Lp protein-1* (*Lpp1*), and demonstrate that its expression pattern is restricted

*To whom correspondence should be addressed. Tel: +44 20 7829 8893; Fax: +44 20 7831 4366; Email: a.copp@ich.ucl.ac.uk

The authors wish it to be known that, in their opinion, the first three authors should be regarded as joint First Authors

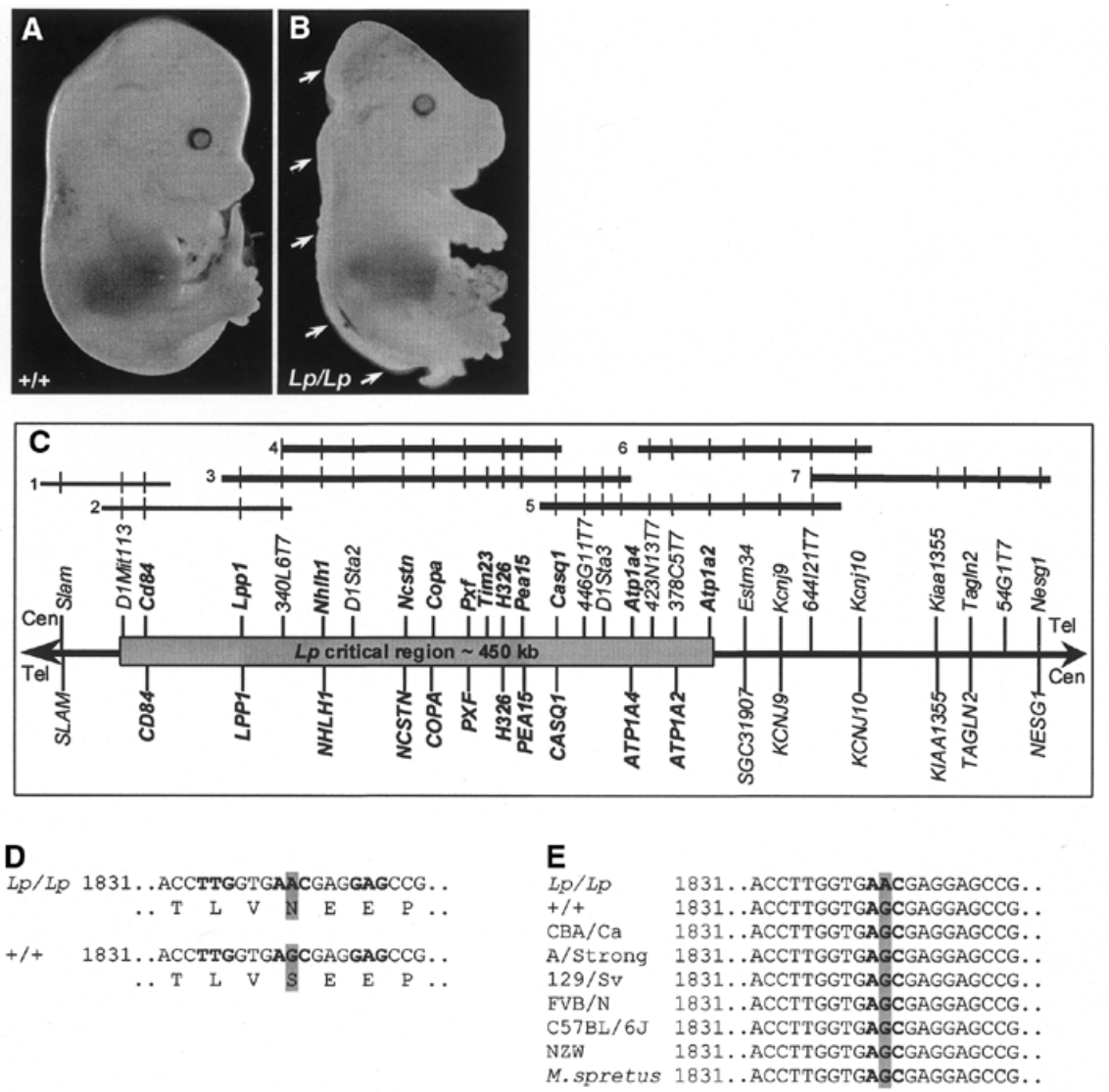

Figure 1. Mutation of *Lpp1* (*Kiaa1215*) in the *Lp* model of severe NTDs. (**A** and **B**) Wild-type and homozygous *Lp/Lp* littermates at E14.5; in craniorachischisis, the neural tube is open from the midbrain throughout the spine (arrows in B). (**C**) Physical map of the *Lp* critical region in mouse and in the homologous region of human 1q22–q23. The mouse critical region is defined by recombinations at *D1Mit113* (10,16) and *365AC16* (accession no. G68177), a microsatellite within the *Atp1a2* gene. Upper part of figure: PAC and BAC clones mapped to the region, with vertical bars indicating the presence of a gene or DNA marker. Thick lines indicate clones that yielded sequence for analysis. Key to clone identities: 1, RP21-506D24; 2, RP23-558L15; 3, RP23-137I20; 4, RP21-340L6; 5, RP21-365D23; 6, RP23-157J4; 7, RP21-644I21. The most proximal part of the critical region was sequenced in human (accession no. NT-004406). Lower part of figure: transcript maps for mouse (above) and human (below). Twelve genes occur in the *Lp* critical region (shaded box) with conservation of gene content and order between mouse and human, although with opposite orientation in relation to the centromere (Cen). (**D**) *Lpp1* nucleotide and predicted peptide sequences over the region of the mutation (highlighted) in *Lp* (upper) and wild-type (lower). The single nucleotide substitution at base 1841 causes a serine to asparagine substitution (S464N) in *Lp*. (**E**) *Lpp1* nucleotide sequences from nine mouse strains over the region of the *Lp* mutation. Nucleotide 1841 (highlighted) is adenine in *Lp*, but guanine in the other eight strains examined. +/+, wild-type chromosome in the *Lp*-carrying LPT/Le inbred strain.

to the lateral boundary of the floor plate in the neurulation stage embryo. Independent studies confirm the mutation of *Lpp1* in *loop-tail* mice (15), strongly indicating that this gene is indeed essential for the initiation of neurulation.

RESULTS

Previous genetic studies have enabled *Lp* to be mapped within a 1.2 cM (~600 kb) interval on distal mouse chromosome 1, between the markers *D1Mit113* and *Tagln2* (10,16–19). This region has extensive homology to human chromosome 1q22–q23 (20). In order to identify candidate genes, we obtained genomic sequence across the entire region in mouse and human. The mouse sequence led to the identification of new informative microsatellite markers which permitted refinement of the critical region to ~450 kb (Fig. 1C).

Lpp1: a candidate gene for *Lp*

A complete transcript map over the refined Lp critical region was developed using a combination of computational-based gene prediction analysis, exon amplification, comparative sequence analysis and cross-species database searching (10,18). The region contains 12 candidate genes, many of which are expressed in the early neurulation stage embryo

(10,21). Sequence analysis of the 128 coding exons and flanking intronic sequences constituting 10 of the 12 genes (*Nhlh1*, *Ncstn*, *Copa*, *Pxf*, *Tim23*, *H326*, *Pea15*, *Casq1*, *Atp1a4* and *Atp1a2*; Fig. 1C) failed to identify any mutation in *Lp* mutant DNA compared with wild-type. Expression analysis of *Nhlh1*, *Copa*, *Pxf* and *Pea15* also revealed normal expression of these genes in *Lp* homozygotes, providing no evidence for a disturbance of transcriptional regulation (10,21,22). An 11th gene, *Cd84*, is not expressed during neurulation (10), and was excluded from the analysis. In the one remaining candidate gene, we identified a mutation within the protein coding region. This gene was described previously as *Kiaa1215*, from its homology to a human cDNA clone (10), and we have now renamed it *Lpp1*.

Comparative sequence analysis identifies a G→A nucleotide transition at position 1841 in exon 8 of *Lpp1*, which causes a serine to asparagine substitution at codon 464 (Fig. 1D). This substitution is unique to the *Lp* mutant chromosome, and is not seen in eight other normal mouse strains (Fig. 1E). Ser464 is conserved in both mouse and human *Lpp1*, and in the related mouse and human *strabismus/van gogh* (*vang*) genes (Fig. 2B), suggesting a critical functional role for this amino acid. The S464N mutation in *Lp* may disrupt polypeptide folding since asparagine ($–CH_2–C–O–NH_2$) is larger than serine ($–CH_2–OH$). Alternatively, Ser464 is a potential phosphorylation site whose loss may compromise Lpp1 function.

Genomic and protein structures of *Lpp1*

Comparison of genomic and cDNA sequences reveals that the mouse and human *Lpp1* genes both comprise eight exons, and span a genomic interval of ~23 and 28 kb, respectively (Fig. 2A). The mouse *Lpp1* cDNA is 2255 bp, compared to a predicted cDNA of 5333 bp from human *LPP1*, a difference that is caused by variation in the polyadenylation signal used. The putative Lpp1 protein contains four predicted transmembrane domains, generating a type 3a membrane topology, with both N- and C-termini located within the cell cytoplasm. The C-terminal domain contains a putative coiled-coil region, and the last four C-terminal amino acids constitute a PDZ-binding domain (Fig. 2C). The Lpp1 protein lacks a signal peptide but contains a possible nuclear localization signal, and may therefore be a component of the nuclear membrane. The presence of two potential protein-binding motifs in Lpp1 suggests that the C-terminal domain may mediate interaction with putative Lpp1 binding partners. Since the S464N mutation lies between these motifs, it could alter their relative conformation and, thereby, affect function.

Mouse and human *Lpp1* genes are highly conserved, with 89% identity at the nucleotide level and 99% identity at the amino acid level (Fig. 2B). Database searches for related proteins identified *Drosophila van gogh* (23,24), and *Cenorhabditis elegans* hypothetical protein B0410.2. Human and mouse vang proteins are also known (24). All five Lpp1-related proteins contain four putative transmembrane domains and a PDZ-binding domain (Fig. 2B), consistent with shared functional properties.

Lpp1 is expressed at the stage and location of developmental abnormalities in *Lp* mice

Reverse-transcriptase PCR of mouse embryonic RNA reveals that *Lpp1* is expressed as early as E7.5, continuing to at least E16.5, although expression cannot be detected in adult brain (Fig. 3A). Hence, expression begins prior to the stage of onset of neurulation, at which *Lp/Lp* embryos first become morphologically abnormal (2,13).

Whole mount *in situ* hybridization of normal (+/+ or *Lp*/+) and *Lp/Lp* neurulation-stage embryos (E8.5–E9.5) reveals *Lpp1* expression in the developing neural tube (Fig. 3B–G). At E8.5, *Lpp1* is expressed in a domain extending from the embryonic hindbrain to the site of initiation of neural tube closure (arrows in Fig. 3B–E). Moreover, sections reveal *Lpp1* expression in a ventro-dorsal gradient within the neural plate (Fig. 3H and I). Wild-type and *Lp*/+ embryos express *Lpp1* within the presumptive floor plate at this stage, whereas *Lp/Lp* embryos exhibit an enlarged floor plate region that is negative for *Lpp1* (compare Fig. 3H and I). Hence, the earliest appearance of an enlarged floor plate in *Lp/Lp* embryos, at the stage when neurulation fails (2,13), is associated with down-regulation of *Lpp1* in this region. By E9.5, the floor plate is negative for *Lpp1* expression in both +/+ and *Lp/Lp* embryos (Fig. 3J and K). Exclusion of the mutated *Lpp1* transcript from the markedly enlarged floor plate of *Lp/Lp* embryos (Fig. 3K) creates a 'split' domain of expression in *Lp/Lp* embryos (Fig. 3L and M). Diminution of *Lpp1* expression dorsally is accentuated in the neural tube of *Lp/Lp* embryos compared to wild-type (Fig. 3K and data not shown), perhaps indicating early degenerative changes in the exposed *Lp/Lp* neuroepithelium.

At post-neurulation stages, *Lpp1* is expressed in a number of tissues in addition to the neural tube. These sites of expression correlate closely with known developmental defects in *Lp/Lp* embryos. Approximately 50% of heterozygous *Lp*/+ mice exhibit an imperforate vagina (7), and we find *Lpp1* expression specifically in the epithelia of the urethra and lower müllerian duct (Fig. 3N), which interact during development of the cervix and vagina. Formation and fusion of the eyelids is absent from *Lp/Lp* embryos (11), while *Lpp1* is expressed in the outer eyelid epithelium, and at the site of eyelid fusion (Fig. 3O). In the heart, *Lpp1* is expressed strongly in the right ventricular outflow tract (Fig. 3P), in close correlation with our recent finding of malalignment of the outflow vessels in *Lp/Lp* mice (25). We also detect expression of *Lpp1* in the developing otocyst and, at later stages, in the cochlea (Fig. 3Q), in agreement with the finding of abnormal inner ear development in *Lp/Lp* embryos (26,27).

Evidence for an interaction between *Lpp1* and *Shh* in defining the floor plate boundary

To investigate the relationship between the expression domains of *Lpp1* and the floor plate marker *Shh*, we hybridized adjacent sections of wild-type embryos with probes for *Lpp1* and *Shh* (Fig. 4A–D). Soon after neural tube closure, at E9.5, when *Shh* is expressed only in the notochord (Fig. 4B), *Lpp1* already exhibits reduced expression in the early floor plate, compared with the rest of the neural tube (Fig. 4A). By E10.5, *Shh* has begun to be expressed in the floor plate. Its domain of expression is complementary to *Lpp1*, which is expressed in the ventral neural tube, but absent from floor plate cells that express *Shh* (Fig. 4C and D). Hence, *Lpp1* and *Shh* exhibit mutually exclusive expression domains in the ventral neural tube.

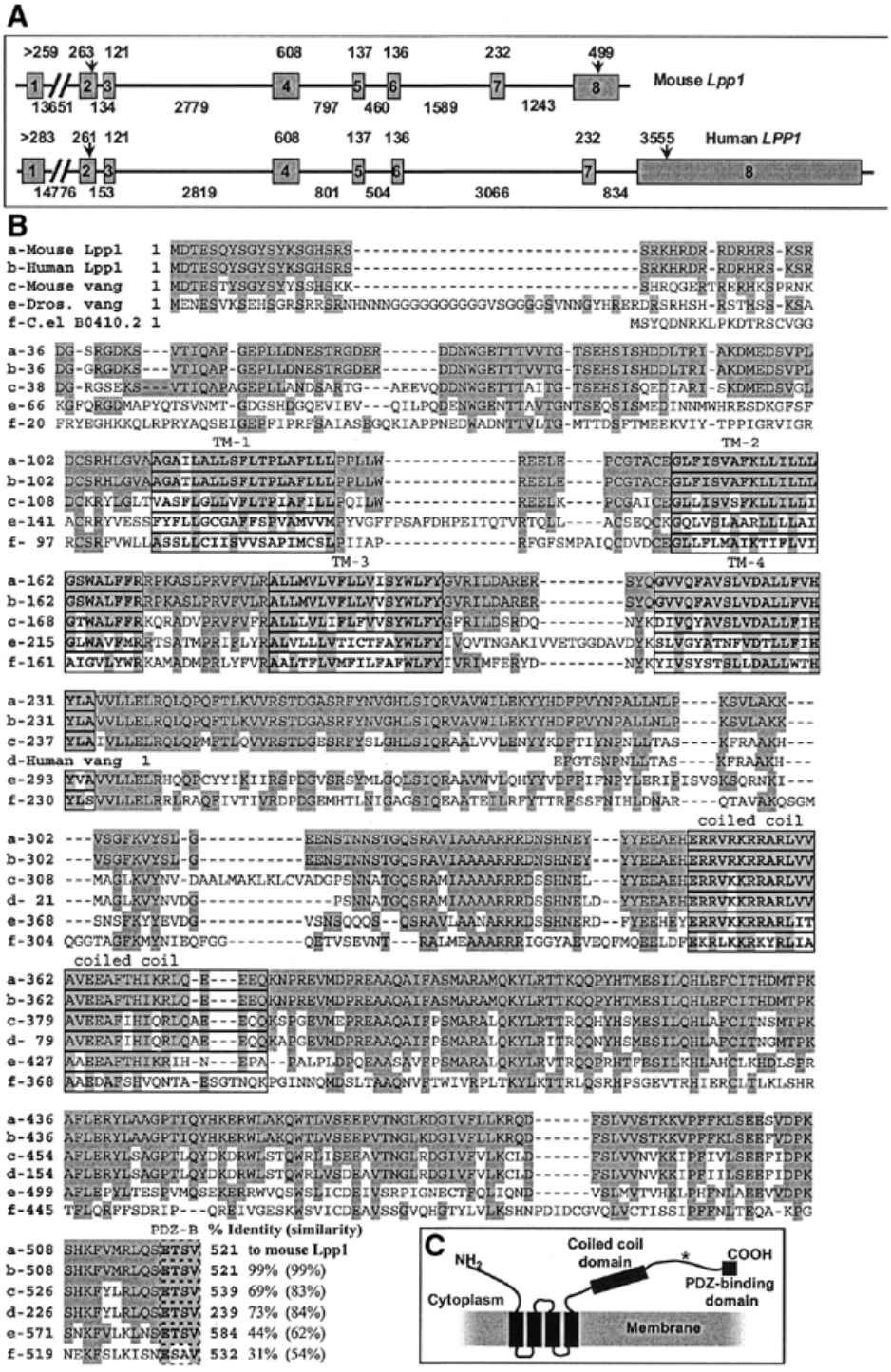

Figure 2. Structure of *Lpp1* gene and protein, compared with orthologues and closely related genes. (**A**) Exon–intron structure of mouse *Lpp1* (upper) and human *LPP1* (lower), previously known as cDNAs *Kiaa1215* and KIAA1215 (10). Boxes represent exons, numbers above each line indicate exon size, and numbers below the line show intron size (bp). Start and end of coding sequence are marked by arrows. (**B**) Predicted peptide sequences of mouse (accession no. AY035370) and human (accession no. AB033041) *Lpp1* genes and comparison with human, mouse (24) and *Drosophila* vang proteins (accession no. AF044208) and with *C.elegans* hypothetical protein B0410.2 (accession no. T15354). Amino acids identical to mouse Lpp1 are highlighted; percentage identity and similarity between mouse Lpp1 and the other proteins is shown at the end of the sequences. Human vang sequence (d) is incomplete and begins half-way down the figure. Each protein contains four putative transmembrane domains (TM), a coiled coil domain and a potential PDZ-binding domain. (**C**) Predicted Lpp1 protein secondary structure; the site of S464N mutation is indicated by an asterisk.

To determine whether *Shh* may negatively regulate *Lpp1* expression in the ventral neural tube, we examined embryos homozygous for a null mutation in the *Shh* gene (28). In E9.5 $Shh^{-/-}$ embryos, *Lpp1* transcripts are detected throughout the neural tube, with no exclusion from ventral midline cells (Fig. 4E and F). This finding is consistent with an absence of

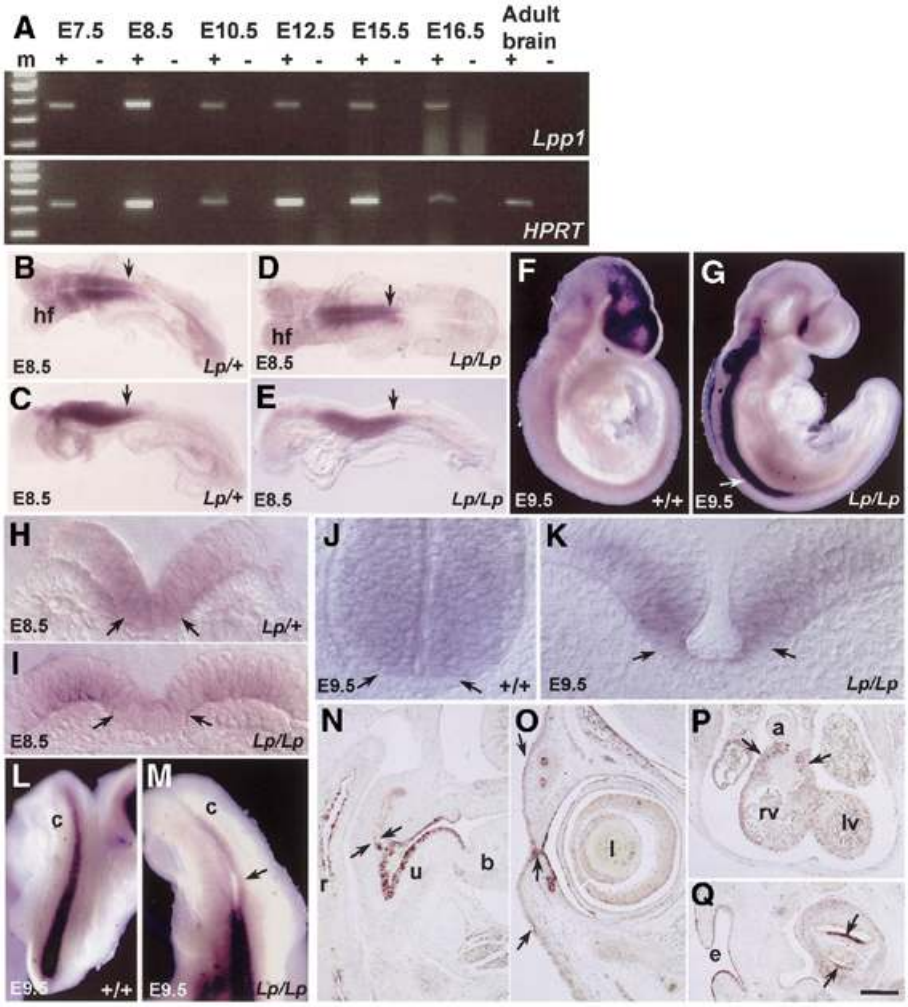

Figure 3. *Lpp1* gene expression in wild-type, *Lp/+* and *Lp/Lp* embryos and fetuses. (**A**) RT–PCR analysis detects *Lpp1* expression in wild-type from E7.5 to E16.5, but not in adult brain. +, RT; −, no RT control. (**B**–**M**) Whole mount *in situ* hybridization for *Lpp1* mRNA at E8.5 (7–8 somite stage) and E9.5 in normally developing (+/+ or *Lp/+*) and *Lp/Lp* embryos (n = 3 for each group). +/+ and *Lp/+* embryos gave identical expression patterns. Whole mounts (B–G) show *Lpp1* expression at E8.5 as a midline stripe extending from the midbrain to the upper spinal region, with intensity of expression declining in a rostro-caudal direction. *Lpp1* is expressed from the hindbrain to the occipital region, where neural tube closure is initiated (arrows in B–E). By E9.5, *Lpp1* expression has extended further into the brain and along most of the spine (F and G). Apparently stronger expression in *Lp/Lp* embryo (arrow in G) is artifactual, owing to the open neural tube. Sections of E8.5 whole mounts at the level of closure initiation show *Lpp1* expression in a ventro-dorsal gradient, with absence of expression from dorsal most neural plate (H and I). Presumptive floor plate expresses *Lpp1* in the *Lp/+* embryo, whereas the markedly broader floor plate of *Lp/Lp* embryos is negative for *Lpp1* (compare regions between arrows in H and I). At E9.5, the floor plate region is *Lpp1*-negative in both +/+ and *Lp/Lp* embryos (between arrows in J and K). Note enlarged floor plate in *Lp/Lp*. (**L** and **M**) E9.5 embryos, from a dorsal view, to show the 'split' in *Lpp1* expression in the *Lp/Lp* embryo (arrow in M). (**N**–**Q**) *In situ* hybridization on sections of wild-type fetuses detects *Lpp1* expression in the urethra and forming vaginal epithelium of the female reproductive tract at E16.5 (arrows in N), in the outer eyelid epithelium and site of eyelid fusion at E15.5 (arrows in O), in the right ventricular outflow tract of the E12.5 heart (arrows in P), and in the cochlea of the inner ear at E14.5 (arrows in Q). Abbreviations: a, aorta; b, bladder; c, caudal region; e, external ear; hf, head fold; lv, left ventricle; r, rectum; rv, right ventricle; u, urethra.

floor plate differentiation in the $Shh^{-/-}$ neural tube (28), and supports the idea that *Lpp1* expression is negatively regulated by *Shh* signalling.

DISCUSSION

In the present study, we have identified a mutation in a previously unknown gene, named *Lpp1*, that may be responsible for the craniorachischisis phenotype in the mouse mutant *loop-tail*. Moreover, we have demonstrated expression of *Lpp1* at diverse sites of developmental abnormality in *Lp/Lp* mice, including an expression domain in the ventral neural tube at the site of initial neural tube closure, which fails in *Lp* mutants. This expression domain is complementary to that of the floor plate marker *Shh*. Altered expression of *Lpp1* in mice lacking Shh suggests a negative influence of Shh on Lpp1 in the ventral neural tube during normal development. Kibar *et al.* (15) have provided independent confirmation that *Lpp1* is the gene mutated in *Lp* mice.

Lpp1 may regulate the lateral extent of floor plate differentiation during neurulation

Midline bending of the neural plate, which marks the site of the presumptive floor plate, depends on an inductive influence of

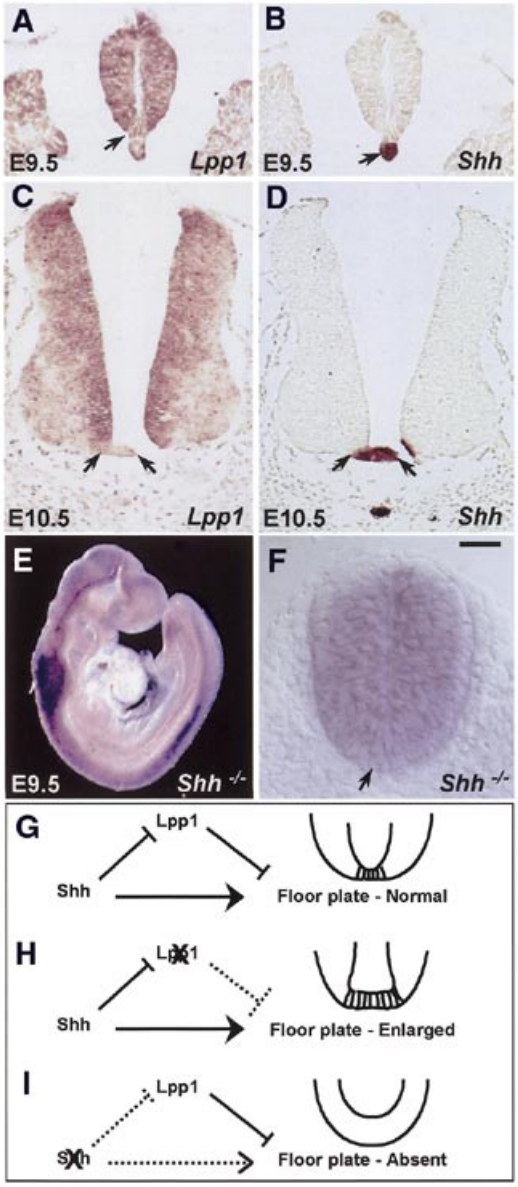

Figure 4. *Lpp1* expression in the neural tube in relation to *Shh* expression. (A–D) Adjacent sections of E9.5 (**A** and **B**) and E10.5 (**C** and **D**) wild-type embryos hybridized for *Lpp1* (A and C) and *Shh* (B and D) expression. At E9.5, the floor plate expresses *Lpp1* at lower intensity than the more dorsal neural tube (arrow in A), at a stage when *Shh* is expressed only in the notochord (arrow in B). At E10.5, *Lpp1* is excluded from the *Shh* expression domain in the floor plate (between arrows in C and D). (**E** and **F**) $Shh^{-/-}$ embryo ($n = 3$), showing uniform expression of *Lpp1* in the dorso-ventral axis of the neural tube. Note the presence of transcripts throughout the ventral part of the neural tube (arrow in F), in contrast to the wild-type appearance (Fig. 3J). (**G–I**) Model to explain the regulation of floor plate development, through interaction between Lpp1 and Shh.

the notochord (29–31), an effect that is partly, but not entirely, dependent on notochordal secretion of Shh peptide (P.Ybot-Gonzalez, P.Cogram, D.Gerrelli and A.J.Copp, submitted for publication). During subsequent development, the floor plate itself becomes a source of Shh, generating a ventral-to-dorsal gradient of Shh influence that patterns neuronal differentiation events along the dorso-ventral axis of the neural tube (32). In *Lp* homozygotes, the presumptive floor plate is enlarged, as judged by the expression of molecular markers including *Shh* and *netrin-1* (13). A similar defect has been observed in human fetuses with craniorachischisis (6), adding weight to the argument that *Lp* represents a useful model of the human NTD condition. The enlarged presumptive floor plate interferes with midline neural plate bending, thereby mechanically inhibiting elevation and apposition of the neural folds, leading to a persistently open neural tube in *Lp/Lp* embryos (13).

We propose that the normal role of *Lpp1* in neurulation may be to restrict the lateral extent of differentiation of the floor plate (Fig. 4G), thereby allowing precisely controlled midline bending of the neural plate, which is necessary for early spinal neural tube closure (14,33). In the absence of functional *Lpp1*, neural plate cells are induced to form floor plate at a greater distance from the ventral midline than normal, leading to the broad floor plate we have observed in *Lp* homozygotes (Fig. 4H). Our findings also suggest that Shh acts as a negative regulator of *Lpp1* expression so that, in the absence of Shh, *Lpp1* expression is detected throughout the ventral neural tube (Fig. 4I). In this respect, *Lpp1* resembles more dorsally located genes such as *Pax3* and *Pax6*, which also show an extension of their expression domains into the ventral neural tube of $Shh^{-/-}$ embryos (28). However, unlike *Lpp1*, loss-of-function mutations in *Pax3* and *Pax6* do not give rise to an enlarged floor plate (13,34), emphasizing the specific relationship of the *Lp* gene product with floor plate development.

Our model of lateral floor plate regulation has several implications. First, the absence of a floor plate in $Shh^{-/-}$ embryos may result not only from the absence of inducing Shh peptide, but also from the presence in the ventral neural tube of inhibitory Lpp1 protein (Fig. 4I). Second, a possible mechanism emerges for the specification of the floor plate boundary. The mutually inhibitory interaction between Lpp1 and Shh at the edge of the floor plate may serve to sharpen the boundary by a mechanism analogous to that suggested for the specification of neuronal territories in the dorso-ventral axis of the neural tube. Here, cross-repression of adjacent homeodomain transcription factors accentuates boundaries established initially through threshold effects of the Shh gradient (35).

Possible molecular interactions involving *Lpp1*

We have demonstrated significant homology at both nucleotide and amino acid levels between *Lpp1* and the *Drosophila* gene *vang*, which acts downstream in the *frizzled/dishevelled* pathway, regulating cell fate and planar polarity, particularly in the eye and wing (23,24). The presence of a PDZ-binding domain indicates a potential interaction with dishevelled, which contains a PDZ domain. In fact, mouse embryos that lack both *dishevelled 1* and *2* function exhibit the defect of craniorachischisis, similar to the phenotype observed in the *Lp/Lp* mutant mouse (A.Wynshaw-Boris, personal communication), providing further support for a role of Lpp1 and dishevelled in a common pathway.

Kibar *et al.* (15) suggest that the *Lp* gene product may participate, with members of the Wnt/Frizzled/dishevelled pathway, in regulating the polarized cell movements of gastrulation and neurulation. Evidence for such a model comes from the findings of convergent–extension defects in amphibian and fish embryos with disturbed function of Wnt11, Frizzled7 and dishevelled (36–38). However, we can find no evidence for a

primary defect of gastrulation during the pathogenesis of *Lp* neurulation defects, making this hypothesis unlikely. For instance, during mouse gastrulation, the node comprises a structure at the anterior end of the primitive streak that contains the precursors of the notochord and floor plate (39,40). Recent studies suggest a normal node structure in pre-neurulation stage *Lp/Lp* embryos (D.Gerrelli and A.J.Copp, unpublished data), consistent with relatively undisturbed gastrulation in *Lp*. Moreover, although the body axis is abnormally short in *Lp/Lp* embryos from neurulation onwards (8), this defect arises only following the failure of Closure 1. Prior to this stage, axial elongation in *Lp/Lp* embryos does not differ from *Lp/+* and *+/+* embryos (9). We prefer an alternative hypothesis: that the primary defect in *Lp* involves abnormal specification of neural plate cells in the midline of *Lp/Lp* embryos, owing to the failure of *Lpp1* to restrict floor plate differentiation to the midline.

Lpp1 and the emerging genetics of NTD

Lpp1 is the first identified gene to be implicated in the causation of craniorachischisis in mammals. Few clues currently exist as to the identity of genes that predispose to human NTD (41). Genes participating in folate metabolism have been studied extensively, in view of the preventive effect of peri-conceptional folic acid administration on the development of human NTD (42,43). An increased risk of NTD has been identified in individuals homozygous for a thermolabile variant of methylene tetrahydrofolate reductase (MTHFR) (44), although this locus is estimated to contribute only a minor proportion of the total genetic risk of NTD (45). Additional genes that play important roles in folate metabolism, including methionine synthase, cystathione β synthase and the folate receptors α and β have not so far been associated with risk of NTD (46). Other studies have concentrated on evaluating human NTD for mutations in genes expressed during mouse neurulation, including some that exhibit NTD when inactivated in knockout mice. As with the folate-related genes, 'developmental' genetic loci have so far not proven to be associated with NTD in a significant proportion of the human cases studied (46).

One possible factor limiting use of the mouse as a guide to the likely nature of human NTD genes is the predominance of recessive genes in mouse NTD; most cases of genetically determined NTD are seen only in homozygous mice while heterozygotes are often phenotypically normal. In contrast, in randomly breeding human populations, NTD cases may be expected to arise most frequently as a result of heterozygosity for one or more predisposing loci. In this context, it is interesting to note that spina bifida occurs at low frequency in *Lp* heterozygotes (2). Moreover, we find that compound heterozygotes between *Lp* and the spina bifida-causing mutation *curly tail* (*ct*) exhibit severe spina bifida, but not craniorachischisis (G.Pavlovska and A.J.Copp, unpublished data), whereas compound heterozygotes for *Lp* and the related mouse NTD gene *Crc* develop craniorachischisis, closely resembling *Lp* homozygotes (12). Hence, in the mouse, *Lpp1* can produce different types of NTD in single heterozygotes and compound heterozygotes with other NTD genes. It will be interesting to determine in future work whether mutations affecting Lpp1 are present in humans with NTD and, if so, whether *LPP1* mutations show a preferential association with craniorachischisis, or may also be present in individuals with spina bifida, anencephaly or other NTD.

MATERIALS AND METHODS

Mouse strains and embryo analysis

Mouse strains A/Strong, CBA/Ca, C57BL/6J, FVB/N and New Zealand White were obtained from Harlan Olac (Bicester, UK), *Mus spretus* and *Shh* gene-targeted mice (28) were obtained from the Mammalian Genetics Unit (Harwell, UK), and LPT/Le, the inbred strain carrying the *Lp* mutation, was originally obtained from the Jackson Laboratory (Bar Harbor, ME). Embryo genotype at the *Lp* locus was determined by use of closely linked SSLP markers by PCR of yolk sac DNA (16), while genotyping of *Shh* knockout mice was as described (28). Noon on the day of finding a copulation plug was designated 0.5 days of embryonic development (E0.5). Pregnant females were killed by cervical dislocation and embryos were dissected from the uterus in Dulbecco's modified Eagle's medium (Gibco BRL, Paisley, UK) containing 10% fetal calf serum, washed in phosphate-buffered saline (PBS) and fixed in 4% paraformaldehyde (PFA) in PBS at 4°C overnight. Embryos were photographed with an SV11 photo-stereomicroscope (Zeiss).

Genomic sequencing and comparative gene sequence analysis

Three mouse PAC clones, RP21-340L6, RP21-365D23 and RP21-644I21, which encompass almost the entire *Lp* critical region, were sequenced at Génoscope (Evry, France). A similar interval is also covered by the genomic sequence generated from the overlapping BAC clones RP23-137I20 (AC074310) and RP23-157J4 (AC074311). The homologous human genomic region has been sequenced as part of the Human Genome Mapping Project (Chr_1ctg82; http://www.sanger.ac.uk/HGP/Chr1/). Comparative sequence analysis of coding exons in *Lp/Lp* and wild-type mice was performed by direct sequencing of PCR-amplified products generated with primers designed to flank each exon (for genomic DNA analysis) or within exons (for cDNA analysis). PCR was performed in 25 µl reaction volumes, with 1× NH_4 buffer (Bioline, UK), 1.0–1.5 mM $MgCl_2$, 0.5 µM forward and reverse primers, 1 U BioPro polymerase (Bioline, UK) and 40 ng of DNA or cDNA. Sequencing reactions were performed with the BIG-dye terminator kit (Perkin Elmer) and analysed on either an ABI-377 or ABI3700 automated sequencer.

Bioinformatics analysis

Genomic sequence was analysed for gene content using the NIX sequence analysis package (available at the HGMP-Resource Centre, Hinxton, UK; http://www.hgmp.mrc.ac.uk/). BLASTN and BLSTX searches (47) were performed using the NCBI web server (http://www.ncbi.nlm.nih.gov/blast/). Protein structure was analysed using the PIX package (available at the HGMP-Resource Centre, Hinxton, UK). Mouse–human genomic comparisons were made by PIP analysis (http://nog.cse.psu.edu/pipmaker/).

Reverse transcriptase PCR

Total RNA was extracted from embryos or adult brain using TRIzol reagent (Life Technologies), according to the manufacturer's instructions. Reverse transcription was performed using ~1–2 µg of total RNA, with 0.2 µg of random hexamers (Life Technologies) and MMLV RT (Life Technologies), following the manufacturer's recommendations. PCR was performed on first-strand cDNA using *Lpp1*-specific primers E1F2 (5′-GATT-GCTTGGTTCTGGGTCC-3′) and E2R2 (5′-GGCACCTT-TAGGAAGTCAAC-3′), which flank intron 1 and therefore generate a 358 bp band from cDNA and >7 kb band from genomic DNA. PCR was performed with 28 cycles, using an annealing temperature of 56°C. RT–PCR control reactions were performed using primers specific for the housekeeping gene HPRT, as described previously (48).

In situ hybridization analysis

Whole mount *in situ* hybridization was performed as described (22). *In situ* hybridization was performed on 8–12 µm paraffin wax sections as described (49). Sense and antisense probes for *Lpp1* were generated by transcription of a 276 bp fragment, corresponding to cDNA region 304–579 bp, (exon 2/exon 3), or a 931 bp fragment, corresponding to cDNA region 560–1490 bp (exon 3/exon 6), cloned into the pGEM-T (Promega) vector. Both probes yielded identical expression patterns for *Lpp1*.

ACKNOWLEDGEMENTS

We thank Deborah Henderson, Nicholas Greene, Gudrun Moore and Radu Aricescu for critical reading of the manuscript and helpful discussions, and Hirva Pota for help with comparative sequence analysis. We are grateful to Richard Evans, Simon Gregory and the Mapping, Sequencing and Clone Resources Group of the Sanger Centre (Hinxton, UK), the UK HGMP Resource Centre (Hinxton, UK), the RZPD (Berlin, Germany) and Génoscope (Evry, France) for assistance with sequencing. This work was supported by grants from SPARKS, Welton Foundation, Medical Research Council, European Union, Birth Defects Foundation and the Wellcome Trust.

REFERENCES

1. Copp, A.J. and Bernfield, M. (1994) Etiology and pathogenesis of human neural tube defects: insights from mouse models. *Curr. Opin. Pediatr.*, **6**, 624–631.
2. Copp, A.J., Checiu, I. and Henson, J.N. (1994) Developmental basis of severe neural tube defects in the *loop-tail* (*Lp*) mutant mouse: use of microsatellite DNA markers to identify embryonic genotype. *Dev. Biol.*, **165**, 20–29.
3. Harding, B.N. and Copp, A.J. (1997) Congenital malformations. In Graham, D.I. and Lantos, P.L. (eds), *Greenfield's Neuropathology*, 6th edn. Arnold, London, UK, pp. 397–533.
4. Seller, M.J. (1987) Neural tube defects and sex ratios. *Am. J. Med. Genet.*, **26**, 699–707.
5. Berry, R.J., Li, Z., Erickson, J.D., Li, S., Moore, C.A., Wang, H., Mulinare, J., Zhao, P., Wong, L.Y.C., Gindler, J., Hong, S.X., Correa, A., China-US Collaborative Project Neu (1999) Prevention of neural-tube defects with folic acid in China. *New Engl. J. Med.*, **341**, 1485–1490.
6. Kirillova, I., Novikova, I., Augé, J., Audollent, S., Esnault, D., Encha-Razavi, F., Lazjuk, G., Attié-Bitach, T. and Vekemans, M. (2000) Expression of the *sonic hedgehog* gene in human embryos with neural tube defects. *Teratology*, **61**, 347–354.
7. Strong, L.C. and Hollander, W.F. (1949) Hereditary loop-tail in the house mouse. *J. Hered.*, **40**, 329–334.
8. Smith, L.J. and Stein, K.F. (1962) Axial elongation in the mouse and its retardation in homozygous looptail mice. *J. Embryol. Exp. Morphol.*, **10**, 73–87.
9. Gerrelli, D. and Copp, A.J. (1997) Failure of neural tube closure in the *loop-tail* (*Lp*) mutant mouse: analysis of the embryonic mechanism. *Dev. Brain Res.*, **102**, 217–224.
10. Doudney, K., Murdoch, J.N., Paternotte, C., Bentley, L., Gregory, S., Copp, A.J. and Stanier, P. (2001) Comparative physical and transcript maps of ~1 Mb around loop-tail, a gene for severe neural tube defects on distal mouse chromosome 1 and human chromosome 1q22–23. *Genomics*, **72**, 180–192.
11. Rachel, R.A., Murdoch, J.N., Beermann, F., Copp, A.J. and Mason, C.A. (2000) Retinal axon misrouting at the optic chiasm in mice with neural tube closure defects. *Dev. Genet.*, **27**, 32–47.
12. Murdoch, J.N., Rachel, R.A., Shah, S., Beermann, F., Stanier, P., Mason, C.A. and Copp, A.J. (2001) *Circletail*, a new mouse mutant with severe neural tube defects: chromosomal localisation and interaction with the *loop-tail* mutation. *Genomics*, in press.
13. Greene, N.D.E., Gerrelli, D., Van Straaten, H.W.M. and Copp, A.J. (1998) Abnormalities of floor plate, notochord and somite differentiation in the *loop-tail* (*Lp*) mouse: a model of severe neural tube defects. *Mech. Dev.*, **73**, 59–72.
14. Shum, A.S.W. and Copp, A.J. (1996) Regional differences in morphogenesis of the neuroepithelium suggest multiple mechanisms of spinal neurulation in the mouse. *Anat. Embryol.*, **194**, 65–73.
15. Kibar, Z., Vogan, K.J., Groulx, N., Justice, M.J., Underhill, D.A. and Gros, P. (2001) *Ltap*, a mammalian homolog of *Drosophila Strabismus/Van Gogh*, is altered in the mouse neural tube mutant Loop-tail. *Nat. Genet.*, **28**, 251–255.
16. Stanier, P., Henson, J.N., Eddleston, J., Moore, G.E. and Copp, A.J. (1995) Genetic basis of neural tube defects: the mouse gene *loop-tail* maps to a region of Chromosome 1 syntenic with human 1q21–q23. *Genomics*, **26**, 473–478.
17. Mullick, A., Trasler, D. and Gros, P. (1995) High-resolution linkage map in the vicinity of the *Lp* locus. *Genomics*, **26**, 479–488.
18. Eddleston, J., Murdoch, J.N., Copp, A.J. and Stanier, P. (1999) Physical and transcriptional map of a three megabase region of mouse chromosome 1 containing the gene for the neural tube defect mutant *loop-tail* (*Lp*). *Genomics*, **56**, 149–159.
19. Underhill, D.A., Mullick, A., Groulx, N., Beatty, B.G. and Gros, P. (1999) Physical delineation of a 700-kb region overlapping the Looptail mutation on mouse chromosome 1. *Genomics*, **55**, 185–193.
20. Seldin, M.F., Morse, H.C., LeBoeuf, R.C. and Steinberg, A.D. (1988) Establishment of a molecular genetic map of distal mouse chromosome 1: further definition of a conserved linkage group syntenic with human chromosome 1q. *Genomics*, **2**, 48–56.
21. Underhill, D.A., Vogan, K.J., Kibar, Z., Morrison, J., Rommens, J. and Gros, P. (2000) Transcription mapping and expression analysis of candidate genes in the vicinity of the mouse Loop-tail mutation. *Mamm. Genome*, **11**, 633–638.
22. Murdoch, J.N., Eddleston, J., Leblond-Bourget, N., Stanier, P. and Copp, A.J. (1999) Sequence and expression analysis of *Nhlh1*: a basic helix–loop–helix gene implicated in neurogenesis. *Dev. Genet.*, **24**, 165–177.
23. Taylor, J., Abramova, N., Charlton, J. and Adler, P.N. (1998) Van Gogh: a new *Drosophila* tissue polarity gene. *Genetics*, **150**, 199–210.
24. Wolff, T. and Rubin, G.M. (1998) Strabismus, a novel gene that regulates tissue polarity and cell fate decisions in *Drosophila*. *Development*, **125**, 1149–1159.
25. Henderson, D.J., Conway, S.J., Greene, N.D.E., Gerrelli, D., Murdoch, J.N., Anderson, R.H. and Copp, A.J. (2001) Cardiovascular defects associated with abnormalities in midline development in the *loop-tail* mouse mutant. *Circ. Res.*, **89**, 6–12.
26. Deol, M.S. (1966) Influence of the neural tube on the differentiation of the inner ear in the mammalian embryo. *Nature*, **209**, 219–220.
27. Wilson, D.B. (1983) Early development of the otocyst in an exencephalic mutant of the mouse. *Acta Anat.*, **117**, 217–224.
28. Chiang, C., Litingtung, Y., Lee, E., Young, K.E., Corden, J.L., Westphal, H. and Beachy, P.A. (1996) Cyclopia and defective axial patterning in mice lacking *Sonic hedgehog* gene function. *Nature*, **383**, 407–413.
29. Van Straaten, H.W.M., Hekking, J.W.M., Wiertz-Hoessels, E.J.L.M., Thors, F. and Drukker, J. (1988) Effect of the notochord on the differentiation of a floor plate area in the neural tube of the chick embryo. *Anat. Embryol.*, **177**, 317–324.

30. Smith, J.L. and Schoenwolf, G.C. (1989) Notochordal induction of cell wedging in the chick neural plate and its role in neural tube formation. *J. Exp. Zool.*, **250**, 49–62.
31. Placzek, M., Tessier-Lavigne, M., Yamada, T., Jessell, T. and Dodd, J. (1990) Mesodermal control of neural cell identity: floor plate induction by the notochord. *Science*, **250**, 985–988.
32. Jessell, T.M. (2000) Neuronal specification in the spinal cord: inductive signals and transcriptional codes. *Nat. Rev. Genetics*, **1**, 20–29.
33. Ybot-Gonzalez, P. and Copp, A.J. (1999) Bending of the neural plate during mouse spinal neurulation is independent of actin microfilaments. *Dev. Dyn.*, **215**, 273–283.
34. Ericson, J., Rashbass, P., Schedl, A., Brenner-Morton, S., Kawakami, A., Van Heyningen, V., Jessell, T.M. and Briscoe, J. (1997) Pax6 controls progenitor cell identity and neuronal fate in response to graded shh signaling. *Cell*, **90**, 169–180.
35. Briscoe, J., Pierani, A., Jessell, T.M. and Ericson, J. (2000) A homeodomain protein code specifies progenitor cell identity and neuronal fate in the ventral neural tube. *Cell*, **101**, 435–445.
36. Heisenberg, C.P., Tada, M., Rauch, G.J., Saúde, L., Concha, M.L., Geisler, R., Stemple, D.L., Smith, J.C. and Wilson, S.W. (2000) Silberblick/Wnt11 mediates convergent extension movements during zebrafish gastrulation. *Nature*, **405**, 76–81.
37. Wallingford, J.B., Rowning, B.A., Vogeli, K.M., Rothbächer, U., Fraser, S.E. and Harland, R.M. (2000) Dishevelled controls cell polarity during *Xenopus* gastrulation. *Nature*, **405**, 81–85.
38. Djiane, A., Riou, J.F., Umbhauer, M., Boucaut, J.C. and Shi, D.L. (2000) Role of *frizzled 7* in the regulation of convergent extension movements during gastrulation in *Xenopus laevis*. *Development*, **127**, 3091–3100.
39. Sulik, K., Dehart, D.B., Inagaki, T., Carson, J.L., Vrablic, T., Gesteland, K. and Schoenwolf, G.C. (1994) Morphogenesis of the murine node and notochordal plate. *Dev. Dyn.*, **201**, 260–278.
40. Davidson, B.P., Kinder, S.J., Steiner, K., Schoenwolf, G.C. and Tam, P.P.L. (1999) Impact of node ablation on the morphogenesis of the body axis and the lateral asymmetry of the mouse embryo during early organogenesis. *Dev. Biol.*, **211**, 11–26.
41. Harris, M.J. (2001) Why are the genes that cause risk of human neural tube defects so hard to find? *Teratology*, **63**, 165–166.
42. Wald, N., Sneddon, J., Densem, J., Frost, C. and Stone, R.; MRC Vitamin Study Research Group (1991) Prevention of neural tube defects: results of the Medical Research Council Vitamin Study. *Lancet*, **338**, 131–137.
43. Czeizel, A.E. and Dudás, I. (1992) Prevention of the first occurrence of neural-tube defects by periconceptional vitamin supplementation. *New Engl. J. Med.*, **327**, 1832–1835.
44. Van der Put, N.M.J., Steegers-Theunissen, R.P.M., Frosst, P., Trijbels, F.J.M., Eskes, T.K.A.B., Van den Heuvel, L.P., Mariman, E.C.M., Den Heyer, M., Rozen, R. and Blom, H.J. (1995) Mutated methylenetetrahydrofolate reductase as a risk factor for spina bifida. *Lancet*, **346**, 1070–1071.
45. Shields, D.C., Kirke, P.N., Mills, J.L., Ramsbottom, D., Molloy, A.M., Burke, H., Weir, D.G., Scott, J.M. and Whitehead, A.S. (1999) The 'thermolabile' variant of methylenetetrahydrofolate reductase and neural tube defects: an evaluation of genetic risk and the relative importance of the genotypes of the embryo and the mother. *Am. J. Hum. Genet.*, **64**, 1045–1055.
46. Juriloff, D.M. and Harris, M.J. (2000) Mouse models for neural tube closure defects. *Hum. Mol. Genet.*, **9**, 993–1000.
47. Altschul, S.F., Madden, T.L., Schaffer, A.A., Zhang, J., Zhang, Z., Miller, W. and Lipman, D.J. (1997) Gapped BLAST and PSI-BLAST: a new generation of protein database search programs. *Nucleic Acids Res.*, **25**, 3389–3402.
48. Melton, D.W., Konecki, D.S., Brennand, J. and Caskey, C.T. (1984) Structure, expression, and mutation of the hypoxanthine phosphoribosyltransferase gene. *Proc. Natl Acad. Sci. USA*, **81**, 2147–2151.
49. Breitschopf, H., Suchanek, G., Gould, R.M., Colman, D.R. and Lassmann, H. (1992) *In situ* hybridization with digoxigenin-labeled probes: sensitive and reliable detection method applied to myelinating rat brain. *Acta Neuropathol.*, **84**, 581–587.